Role of the Zeolitic Environment in Catalytic Activation of Methanol

I. Štich,*,†,‡ J. D. Gale,§ K. Terakura,¶,⊥ and M. C. Payne‖

Contribution from JRCAT, Angstrom Technology Partnership (ATP), 1-1-4 Higashi, Tsukuba, Ibaraki 305-0046, Japan, Department of Physics, Slovak Technical University (STU), Ilkovičova 3, SK-812 19, Bratislava, Slovakia, Department of Chemistry, Imperial College of Science, Technology and Medicine, South Kensington, London SW7 2AY, U.K., JRCAT, National Institute for Advanced Interdisciplinary Research (NAIR), 1-1-4 Higashi, Ibaraki 305-8562, Japan, CREST, Japan Science and Technology Corporation (JST), Kawaguchi, Saitama 332, Japan, and Cavendish Laboratory, Madingley Road, Cambridge CB3 0HE, U.K.

Abstract: We present an extensive study of the initial stages of the methanol to gasoline conversion in the framework of the ab initio molecular dynamics approach. We investigate the effect of different zeolite environments, methanol loading, and temperature and show that, for understanding the initial adsorption and activation of the adsorbed species, all three factors need to be considered simultaneously. The results allow us to develop a simple model for the activation of the methanol molecule, which elucidates the role of both the zeolite framework and the methanol solvent. The zeolite framework plays an active role in methanol protonation. The solvent significantly softens the C−O bond of the methoxonium, rendering it very anharmonic. High mobility of the methoxonium cation, promoted by some zeolite frameworks, prevents it from forming hydrogen bonds with the active sites and the solvent leading to the activation of the methoxonium species. This picture is shown to be consistent with the experimental infrared spectra.

1. Introduction

One of the most significant industrial applications of zeolites exploits the ability of the microporous aluminosilicate environment to catalyze the methanol to gasoline (MTG) process.[1] The industrial process proceeds at elevated temperatures (∼700 K) and methanol pressures which correspond to a loading of ∼5−6 methanol molecules per acidic hydroxyl group,[2] which is believed to be the active site. The catalyst used for this process is typically ZSM-5. There is a large volume of experimental evidence that the adsorbed methanol is first dehydrated to dimethyl ether (DME) that subsequently reacts with methanol to form hydrocarbons, either directly or via reconversion to methanol. Furthermore, the experiments suggest a dramatic increase by almost 2 orders of magnitude in DME formation in a narrow temperature range around 500 K.[3] However, the nature of methanol adsorption in the zeolite, the mechanism of dehydration, and formation of the C−C bonds in the hydrocarbons are still far from understood.

Methanol is known from infrared spectroscopy (IR)[2] to be initially adsorbed at acid sites in the zeolite framework. Unfortunately, the IR data cannot be unambiguously interpreted as resulting either from a physisorbed methanol complex[4,5]

† ATP.
‡ STU.
§ Imperial College.
¶ NAIR.
⊥ CREST.
‖ Cavendish Laboratory.
(1) Meisel, S. L. et al. *Chem. Technol.* **1976**, *6*, 86.
(2) Mirth, G. et al. *J. Chem. Soc., Faraday Trans.* **1990**, *86*, 3039.
(3) Wakabayashi, F. et al. *Stud. Surf. Sci. Catal.* **1996**, *105*, 1739.
(4) Anderson, M. W.; Klinowski, J. *J. Chem. Soc., Faraday Trans.* **1990**, *112*, 10.
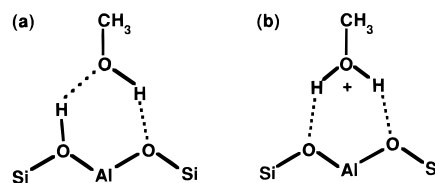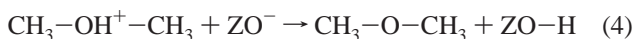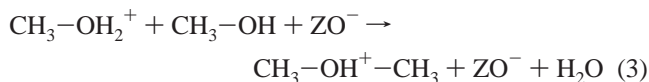(5) Murray, D. K.; Chang, J.-W.; Haw, J. F. *J. Am. Chem. Soc.* **1993**, *118*, 4732.

Figure 1. Schematic illustration of the two possible adsorption complexes of methanol at a Brønsted acid site: (a) physisorbed species with weak bonds to the zeolite framework and (b) chemisorbed methoxonium cation ($CH_3-OH_2^+$) involving the transfer of a zeolitic proton.

(Figure 1a) or from a chemisorbed complex[2,6] (Figure 1b), in which case a methoxonium cation ($CH_3^-OH_2^+$) is formed. For the dehydration process two different mechanisms have been proposed. In the indirect pathway[7,8] the methyl group is first adsorbed on the acid site

$$CH_3-OH_2^+ + ZO^- \rightarrow ZO-CH_3 + H_2O \qquad (1)$$

which subsequently reacts with the other methanol molecule

$$CH_3-OH + ZO-CH_3 \rightarrow CH_3-O-CH_3 + ZO-H \quad (2)$$

Here Z stands for the zeolite framework. We assume here that the methanol is chemisorbed at an acid site as the protonated complex is expected to be more susceptible to nucleophilic attack. Alternatively, in the direct pathway[9]

(6) Pope, C. G. *J. Chem. Soc., Faraday Trans.* **1993**, *89*, 1139.
(7) Ono, Y.; Mori, T. *J. Chem. Soc., Faraday Trans.* **1981**, *77*, 2209.
(8) Forester, T. R.; Howe, R. F. *J. Am. Chem. Soc.* **1987**, *109*, 5076.
(9) Bandiera, J.; Nacchache, C. *Appl. Catal.* **1991**, *69*, 139.

$$CH_3-OH_2{}^+ + CH_3-OH + ZO^- \rightarrow$$
$$CH_3-OH^+-CH_3 + ZO^- + H_2O \quad (3)$$

$$CH_3-OH^+-CH_3 + ZO^- \rightarrow CH_3-O-CH_3 + ZO-H \quad (4)$$

both methanol molecules react with each other inside the zeolite environment, which acts merely as a solvent. Additionally there are competing pathways in which methanol reacts to form a carbon—carbon bond, such as in producing ethanol. However, the activation energy for this process has been shown to be much higher than that for formation of dimethyl ether.[10]

Recently theoretical studies[11-13] have started to shed light on the initial stages of the MTG process. The first studies used very small clusters containing of the order of 10 atoms to model adsorption of a single methanol molecule at an acid site and reached the conclusion that methanol was only physisorbed.[14-16] Later calculations, which used embedding of these small clusters into point charge fields to emulate the electrostatic potential of the zeolite cavity, showed that the lattice increases the tendency for proton transfer to occur.[17] The role of the lattice in the adsorption process was further underlined in very recent calculations[18,20,21] which used periodic boundary conditions with the full zeolite topology. These calculations indicated that the type of zeolite framework may play a role in the nature of the initial adsorption and that both types of adsorption may occur. In addition, these studies[13] also give a strong support to the direct reaction of methanol (reactions 3 and 4) as the preferred pathway. Following the tradition in this field, the focus was on local properties, such as location of the reaction intermediates and transition states. However, these studies have also raised a number of questions about the role of the proton transfer and zeolite catalysts in methanol activation, namely, (I) the microporous zeolitic environment was found to increase the endothermicity of reactions 3 and 4 compared to the reaction in the gas phase and (II) all previous calculations suggested very little change in the methanol/methoxonium geometries on adsorption in the zeolite or after protonation of methanol in a vacuum.[13,18]

The goal of the present paper is to resolve these issues and in particular to explore the factors which are known to be important in the industrial MTG process and have not been considered in previous studies. The factors we consider are as follows: (1) full zeolite topology and the effect of different zeolite environments; (2) methanol loading; and (3) finite temperature effects and the concomitant dynamical effects. The last factor is important because it is now accepted that the energy barriers for the proton transfer reaction are of the order of thermal energies. Hence the system will explore several minima on the potential energy surface (PES), which are likely be very anharmonic and sensitive to the low-frequency vibrations of the

encapsulating framework.[19] We show that (1)−(3) are the minimum ingredients required for understanding the catalytic action of zeolites. Indeed, these calculations are the first to show any activation of methanol in a zeolite catalyst. In the present study we use ab initio (in the framework of the density functional theory (DFT)) molecular dynamics (MD) simulation.[22] We believe that this technique is currently the only method that has sufficient accuracy and is capable of *simultaneously* including *all* the above factors. The efficiency of this approach is demonstrated by performing the first ab initio MD calculations for the true catalyst, namely ZSM-5. The unit cell of ZSM-5 has 288 atoms which represents a tremendous computational challenge. Only a single-point ($T = 0$ K) HF calculation with a minimal basis set currently exists in the literature for this system.[23] This is due to the computational cost associated with the loss of space group symmetry that results from inclusion of the aluminum defect and from the thermal motion of the atoms as well as due to the need to follow the system dynamics over a large number of atomic configurations.

In addition, we also assess the importance of the quantum corrections to the behavior of the zeolitic proton. As shown below, the PES for the proton transfer reaction has a double-well form with a rather low energy barrier. In such a situation quantum fluctuations may become important. For this purpose we augment our first-principles MD method with a path-integral (PI) description of the protons.[24,25] We note in passing that treatment of the quantum dispersion effects in the harmonic approximation is not appropriate in the present case due to the flatness of the PES and strongly anharmonic behavior.

Our main results may be summarized as follows: (a) A single methanol molecule may be both physisorbed and chemisorbed, depending on the zeolite catalyst; (b) As soon as the methanol loading is increased to two molecules per acid site we invariably observe chemisorbed methoxonium species; (c) Existence of the methoxonium species alone is *insufficient* to produce activation of the adsorbed species and hence represents only a necessary but *not* sufficient condition for activation; (d) Methanol solvent significantly softens the methoxonium C—O bond and renders it very anharmonic; (e) At higher methanol loading reducing the hydrogen bonding of the methoxonium cation to the other methanol molecules and to the zeolite channel produces a further weakening of the methoxonium C—O bond leading to its activation. This process is associated with the methoxonium mobility in the zeolite which is promoted by some frameworks; (f) Calculated vibration spectra support the above picture of activation of the methoxonium cation and suggest clustering of methanol molecules around the active site; (g) Quantum dispersion effects for the zeolitic proton at room temperature were not found to significantly alter the picture emerging from the classical treatment of the protons. A short account of part of these results appeared elsewhere.[26]

The rest of the paper is organized as follows. Section 2 describes the most important technical details of the calculations. Our results for the proton transfer, activation of the methanol molecule, and methanol vibrations are presented in Section 3. To convey some impression of the large degree of the anharmonicity of the PES we analyze thermal fluctuations in Appendix A. Appendix B deals with the quantum fluctuations

(10) Blaszkowski, S. R.; van Santen, R. A. *J. Am. Chem. Soc.* **1997**, *119*, 5020.
(11) Blaszkowski, S. R.; van Santen, R. A. *J. Phys. Chem.* **1995**, *99*, 11728.
(12) Blaszkowski, S. R.; van Santen, R. A. *J. Am. Chem. Soc.* **1996**, *118*, 5152.
(13) Shah, R.; Gale, J. D.; Payne, M. C. *J. Phys. Chem.* **1997**, *B101*, 4787.
(14) Haase, F.; Sauer, J. *J. Phys. Chem.* **1994**, *98*, 3083.
(15) Haase, F.; Sauer, J. *J. Am. Chem. Soc.* **1995**, *117*, 3780.
(16) Gale, J. D. *Top. Catal.* **1996**, *3*, 169.
(17) Greatbank, S. P.; Hillier, I. H.; Burton, N. A.; Sherwood, P. *J. Chem. Phys.* **1996**, *105*, 3770.
(18) Shah, R. et al. *Science* **1996**, *B271*, 1395.
(19) Hammonds, K. D. et al. *Phys. Rev. Lett.* **1997**, *78*, 3701.
(20) Nusterer, E.; Blöchl, P. E.; Schwarz, K. *Angew. Chem., Int. Ed. Engl.* **1996**, *35*, 175.
(21) Haase, F.; Sauer, J.; Hutter, *J. Chem. Phys. Lett.* **1997**, *266*, 397.

(22) Payne, M. C. et al. *Rev. Mod. Phys.* **1992**, *64*, 1045.
(23) White, J. C.; Hess, A. C. *J. Phys. Chem.* **1993**, *97*, 8703.
(24) Marx, D.; Parrinello, M. *Z. Phys.* **1994**, *B95*, 143.
(25) Marx, D.; Parrinello, M. *J. Chem. Phys.* **1996**, *104*, 4077.
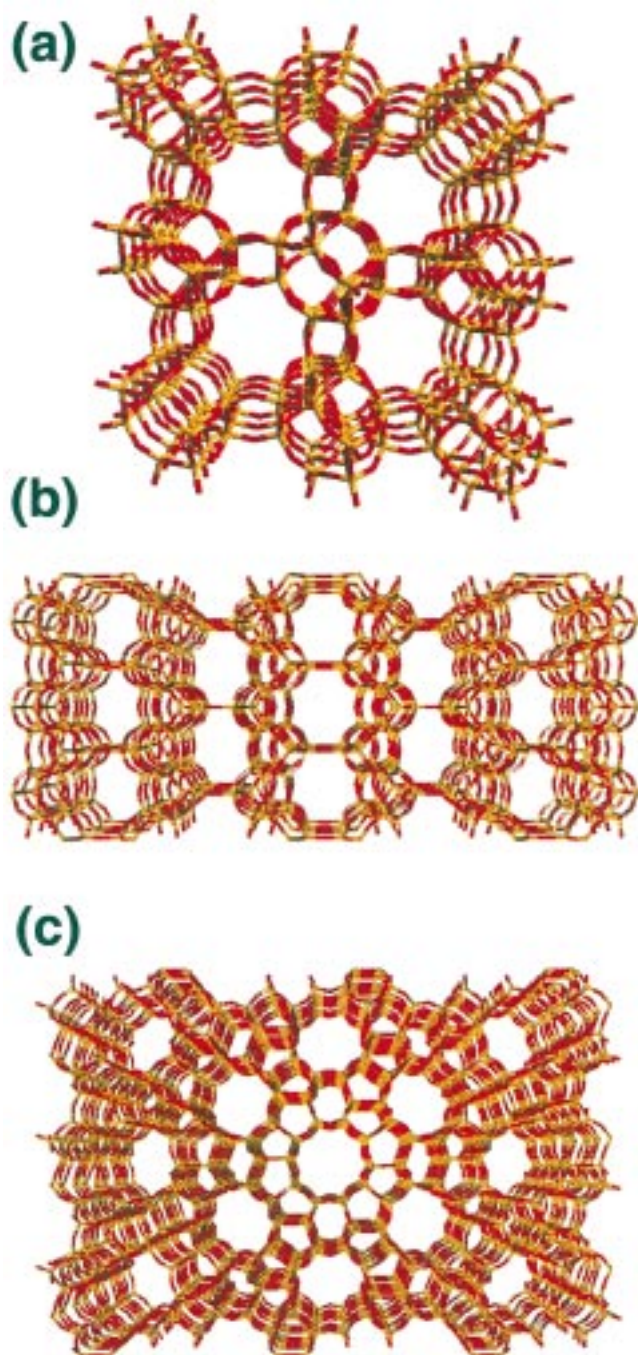(26) Štich, I. et al. *Chem. Phys. Lett.* **1998**, *283*, 402.

Figure 2. Perspective views of the bulk structures for (a) chabazite, (b) ferrierite along the 8-ring channel, and (c) ZSM-5 along the straight channel.

and the PIMD calculations we have performed. Our main findings are summarized in Section 4.

2. Details of Calculations

We have performed an extensive ab initio MD simulation study in order to explore the factors which influence the nature of the adsorbed state of methanol in a zeolitic environment.

We have included three zeolite frameworks for study: chabazite, ferrierite, and ZSM-5, shown in Figure 2. Chabazite[27] (Figure 2a) has a small 36-atom unit cell and a structure that consists of only 8-ring channels. The commercial catalyst ZSM-5[28] (Figure 2c) has two types of 10-ring channels: straight and sinusoidal running at right angles to

each other. We included also ferrierite[29] (Figure 2b) in the study, which has a structure very similar to ZSM-5, as it has 10-ring channels along one direction, similar to those in ZSM-5, but with a much smaller (54-atom) unit cell. Ferrierite, however, also has another type of straight channel, with an 8-ring aperture, perpendicular to the 10-ring channels. Chabazite was included in order to draw comparisons with the previous static calculations,[18,13] whereas ferrierite was used as the smallest close mimic to the true catalyst ZSM-5. We assume in these calculations that the Brønsted acid sites are independent and we consider the presence of just a single acid site per unit cell. The location of the acid site in the unit cell requires some attention with regard to placement of the Al defect and the charge-neutrality compensating zeolitic proton. In chabazite, all possible Al placements are equivalent, which is not true in ferrierite and ZSM-5. As we cannot explore the PES for all the possible placements of the Brønsted site, in ferrierite (ZSM-5) we have placed Al on T4 (T12) and the proton initially on O6 (O24). This means that the acid site is located at the intersection of the two channels. The initial placement of the proton is not critical as this proton is mobile on a fraction of the time-scale of our simulations. Given the high flexibility of the zeolite framework, which in our calculation is allowed to fully respond and relax, we believe that there is little difference between the different tetrahedral sites and that the choice made here has little effect on the results presented.

The electronic structure part of the simulations was performed within the DFT framework in the plane-wave pseudopotential formulation.[22] The local density approximation for the exchange-correlation functional has been shown to be inadequate for description of reactions which involve proton transfer[30] and we have used the PW91[31] form of the gradient corrected functional. We treat explicitly the valence electrons and use pseudopotentials to represent the core electrons. For O and C we employ optimized-Q_c filter tuned-pseudopotentials.[32] Conventional Kerker-type[33] pseudopotentials are used for Si and Al and a bare Coulomb potential for H. The electronic states are expanded in a plane-wave basis set at a single k-point (Γ-point) in the Brillouin zone. The accuracy of the method was verified at an energy cut-off of $\sim$47 Ryd both in the solid-state limit (reproduction of the lattice parameter of α quartz) and in the molecular limit (structure of the methanol molecule to within $\sim$0.01 Å and proton affinity to within 4 kJ/mol).[18] The present calculations have been done at a slightly smaller cut-off of $\sim$ 40 Ryd, but the effect on the results was found to be negligible.

All simulations (we defer the details of the PIMD simulations to Appendix B) have been performed in the canonical (N,V,T) ensemble. We use a time step of $\sim$0.6 fs in the discretization of the ionic dynamics with all atoms allowed to move. We work within the Born–Oppenheimer (BO) approximation and at each MD step the energy is converged back to the BO surface with a very high accuracy of 10^{-6} eV/atom using conjugate gradient methods.[34] This accuracy is required because of the flatness of the BO surface. The methanol loading was studied in the range of 1 to 4 per acid site. All simulations have been performed at room temperature, with one simulation at $T = 700$ K to emulate the effect of reaction conditions. Given the very high computational cost[35] of the ab initio MD, dynamical simulations are possible only on a picosecond time scale. The typical time scale used in the present simulations was between 4 and 6 ps, except for the simulation in ZSM-5, where only 1.3 ps was feasible. Our recent transition state search for the formation of DME from two methanols in chabazite found a total energy barrier of 0.7 eV.[36] Clearly, our MD

(27) Dent, L. S.; Smith, J. V. *Nature* **1958**, *181*, 1794.

(28) van Konigsveld, H.; van Bekkum, H.; Jansen, J. C. *Acta Crystallogr.* **1987**, *B43*, 127. Note that we use the orthorhombic structure that is more appropriate at room temperature than the low-temperature monoclinic form.

(29) Vaughan, P. A. *Acta Crystallogr.* **1966**, *21*, 983.

(30) Blaszkowski, S. R. et al. *J. Phys. Chem.* **1994**, *98*, 12938.

(31) Perdew, J. P. et al. *Phys. Rev.* **1992**, *B46*, 6671.

(32) Lee, M.-H. Thesis 1995, University of Cambridge, UK.

(33) Kerker, G. P. *J. Phys.* **1980**, *C13*, L189.

(34) The algorithm is closely related to the conjugate-gradient algorithms described in: Štich, I. et al. *Phys. Rev.* **1989**, *B39*, 4997; Gillan, M. J. *J. Phys. Condens. Matter* **1989**, *1*, 689.

(35) We use parallel computing in the spirit described in: Clarke, L. J.; Štich, I.; Payne, M. C. *Comput. Phys. Commun.* **1992**, *72*, 14.

(36) Sandré, E.; Payne, M. C.; Štich, I.; Gale, J. D. In *Transition State Modeling for Catalysis*; ACS Symposium Series 721; Truhlar, D. G., Morokuma, K., Eds.; American Chemical Society: Washington, DC.

observation time is too short to observe chemical reactions which involve reaction barriers of this order of magnitude. Hence, all our simulations remain in the reactant basin of the PES. However, as shown below, this MD observation time is sufficient to observe the proton transfer, perform a statistical sampling of the PES on the reactant side, and provide strong indications on the nature of the activation process.

3. Results and Discussion

Our results are based on analyzing up to $\sim 10^4$ configurations for each simulation. To convey the information on the process of methanol protonation and activation we show representative configurations and distributions of the most important bonds, namely the C−O and the O-H bonds of the methanol/ methoxonium molecule(s). Vibrational properties of those bonds are compared with results from IR spectroscopy. The results are used to develop a simple model of methanol activation elucidating the role of both the zeolite framework and the methanol solvent.

Single methanol calculations have been performed for all three zeolite frameworks. We discuss these results first to show that the nature of the initial methanol adsorption depends on the zeolite topology and that the presence or absence of proton transfer is strongly correlated with the degree of spatial constraint due to the zeolite framework. In Figure 3 we show the bond-length distribution of the two hydrogen bonds for methanol adsorbed in the 8- and 10-ring channels of ferrierite, the 8-ring of chabazite, and at the intersection of the two 10-ring channels in ZSM-5. The corresponding methanol C−O bond-length distributions are shown in Figure 4, and the typical adsorption geometries are shown in Figure 5a−c. One can see that the zeolitic proton is clearly transferred to the methanol molecule in both channels in the ferrierite framework. In chabazite the proton resides predominantly on the zeolite framework and in the ZSM-5 the zeolitic proton does not attempt to make even short-lived fluctuations to create a chemical bond with the methanol molecule. The other trend clearly emerging from Figure 3 is the correlation between proton transfer and the extent of zeolitic confinement. There is a noticeable increase in the fraction of physisorbed methanol in otherwise very similar zeolite environments on going from the ferrierite 8-ring to the ferrierite 10-ring and a dramatic increase on going to ZSM-5. This is in line with the amount of free space available to the methanol molecule. In addition, the bond strength of the other proton in the methanol/methoxonium complex is correlated with the fluctuations of the zeolitic proton leading to protonation. These fluctuations destabilize and soften the hydroxyl bond on the methanol molecule, a trend clearly visible in Figure 3.

In ferrierite we have used the primitive unit cell which has a very short unit cell parameter in one direction. This increases the fictitious image-type interaction between the methoxonium cations. Simple analysis shows that the direction of the dipole formed when methanol is adsorbed in the 8-ring is such that this interaction hinders the protonation, while favoring it in the 10-ring. Hence, the differences between the results shown in Figure 3a,b are actually underestimated due to the fictitious image interaction. We have verified this effect by performing an additional simulation in the 8-ring channel using a system where the unit cell was doubled in the short unit cell dimension. Results for proton distributions shown in Figure 6 indicate that the amount of fluctuations corresponding to physisorbed species have been slightly reduced in the doubled unit cell which fully corroborates the above argument. Otherwise the trajectories are rather similar.

The differences we observe in the nature of the adsorbed species are reflected also in the adsorption geometries. For
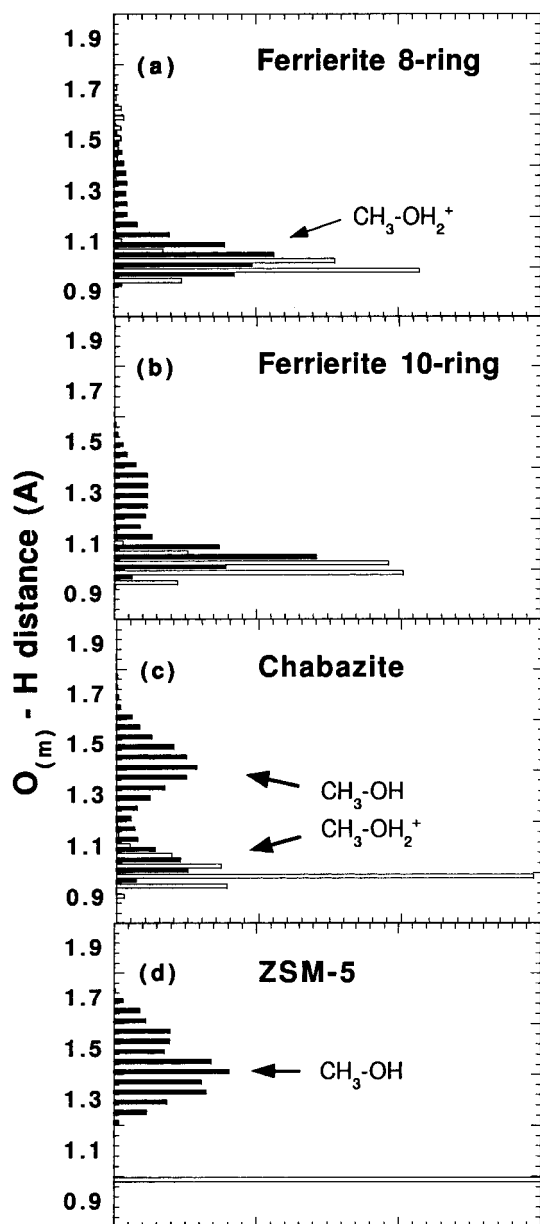

Figure 3. Bond length distributions of the O−H distances for a single methanol adsorbed in (a) the 8-ring channel of ferrierite, (b) the 10-ring channel of ferrierite, (c) chabazite, and (d) ZSM-5. The two distributions in each panel correspond to the two protons.

example, the physisorbed molecule in chabazite is hydrogen bonded (Figure 5b) so as to straddle the acid site, whereas the chemisorbed methoxonium species in the 8-ring channel of ferrierite was initially able to break the weaker H-bonds binding it to the zeolite framework and rotated away from the acid site to find a new geometry (Figure 5a) stable for over 4 ps. During the rotation stage, where there is a significant reduction in the extent of hydrogen bonding, we observed no fluctuations at all which return the proton back onto the framework. They started occurring later in the new adsorption geometry characterized by new H-bonds (Figure 5a). In the 10-ring channel of ferrierite the proton is less tightly transferred and the molecule retains one of the H-bonds to the acid site but rotates partially away from the acid site. This indicates that even for species which are predominantly protonated the strength of the chemical bond of the proton to the methanol molecule depends on the interaction of the protonated complex with the zeolite channel.
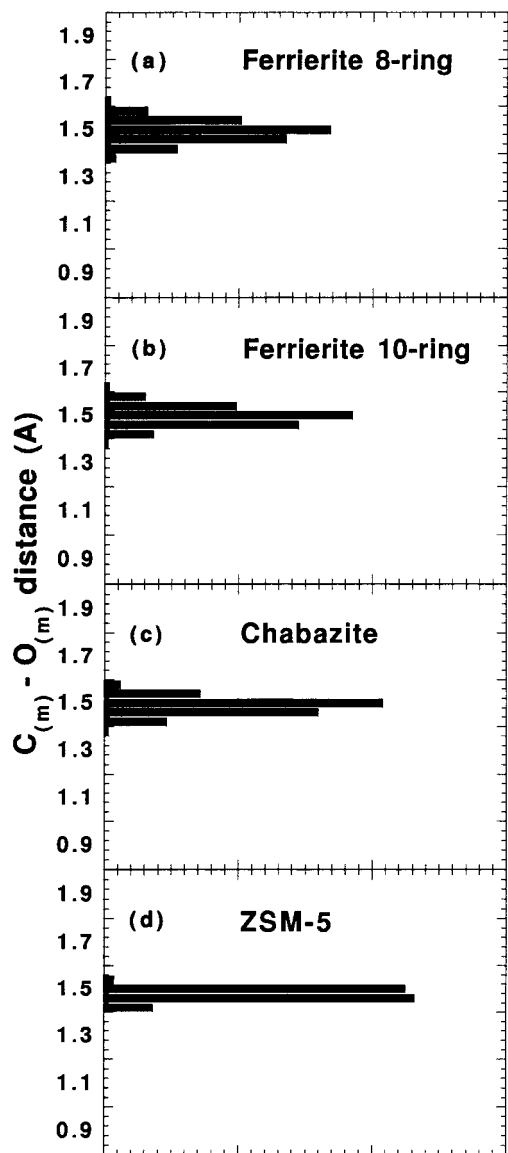
Figure 4. The same as Figure 3 but for the methanol C–O bond.

Figure 5. Selected geometries sampled from the MD trajectories: single methanol adsorption in (a) the 8-ring channel of ferrierite, (b) chabazite, and (c) ZSM-5; two methanol complexes adsorbed in (d) the 8-ring channel of ferrierite and (e) chabazite; and (f) reaction conditions approximated by a four-methanol complex in an 8-ring channel of ferrierite. The aluminum defect is shown in pink, and dashed lines indicate the hydrogen bonds.

The absence of the zeolitic environment with its associated spatial constraints in the simple cluster models of the size customarily used in the past explains the physisorbed methanol species invariably found in those studies.[16] Incidentally, our results for chabazite are also at variance with the results of the previous static optimization which also used the full zeolite topology and found methanol in chabazite to be protonated.[18] As shown in Appendix A, the zeolitic proton executes a motion in a double-well potential with the physisorption well being slightly lower in energy. The static optimization missed the physisorption minimum and located only the local minimum corresponding to chemisorption. The present result is in agreement with the conclusion reached in ref 21 based on ab initio MD simulation. Similarly, the static structural optimization we performed for methanol in the 8-ring of ferrierite yielded an initially physisorbed species. At 300 K, however, proton transfer occurred in ~0.5 ps and the methoxonium cation was the stable species at this temperature. This demonstrates the need of statistical (in the spirit of MD or Monte Carlo) importance sampling of the underlying PES in complex systems such as these.

These results show that even a single methanol molecule may be protonated in the microporous zeolite environment. However,
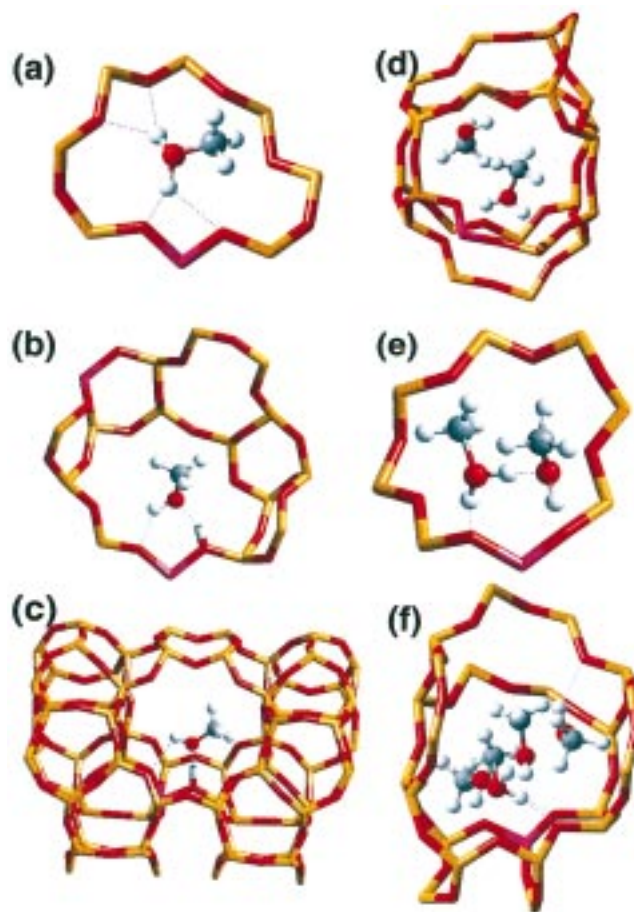
the expectation that this additional hydrogen bond would significantly weaken the C–O bond of the adsorbed methanol and induce activation of the methanol molecule is not born out in the C–O bond length distributions shown in Figure 4. One does observe an increase in the anharmonicity of this bond, but the mean value of the bond length remains the same irrespective of whether the methanol is protonated or not. The other conclusion one can draw is that in this initial stage of the MTG process the environment of the commercial catalyst ZSM-5 does not seem to introduce any new feature that would explain the process of activation of the methanol molecule. Hence, the activation process is either an extremely rare event that cannot be observed on the picosecond time scale or is caused by other factors, not explored so far in our study. The most significant factors where our calculations deviate from the reaction conditions are high methanol loadings and temperatures under reaction conditions. To explore these factors we have performed additional simulations.

Two methanols per acid site loading was studied in both the 8-ring channel of ferrierite and chabazite. The methanol molecules have been initially assumed to form a hydrogen-bonded cluster (Figure 7) with one methanol hydrogen bonded to both zeolite framework and the second methanol molecule and the proton on the acid site. Existence of such adsorption complexes has been conjectured from IR studies.[2] As can be seen in Figure 8, in both structures the proton is lost from the
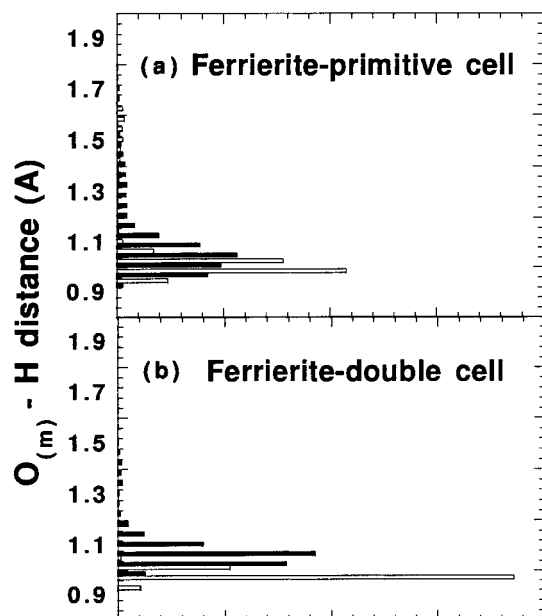
Figure 6. Comparison of results obtained for a single methanol molecule adsorbed in the 8-ring of ferrierite with (a) the primitive unit cell and (b) a cell whose dimension was doubled along the short unit cell axis.
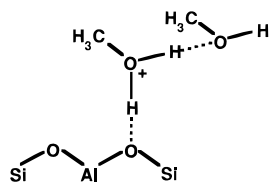

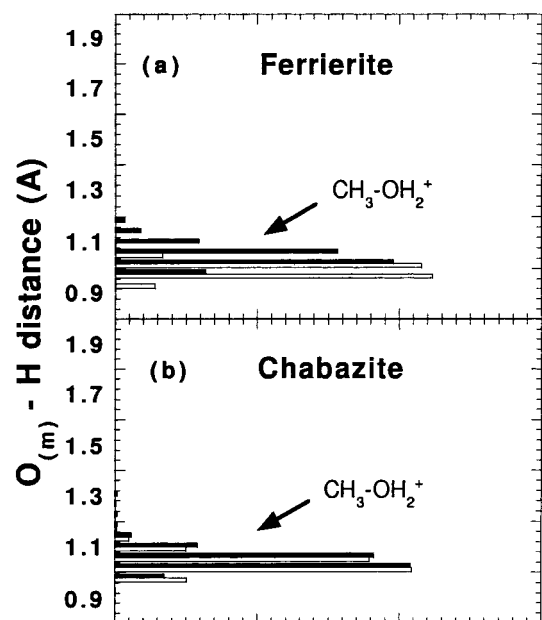**Figure 7.** Schematic illustration of the protonated H-bonded cluster of two methanol molecules.

Figure 8. Bond length distributions of the O-H distances for the methoxonium cation in the two-methanol complexes adsorbed in (a) the 8-ring of ferrierite and (b) chabazite. The two distributions in each panel correspond to the two protons in the methoxonium ion.

framework to methanol and the methoxonium cation remains stable over the entire MD time scale.[37] This is clearly visible in Figures 5, parts d and e. The methanol solvent causes a very significant softening of the PES along the methoxonium $C-O$
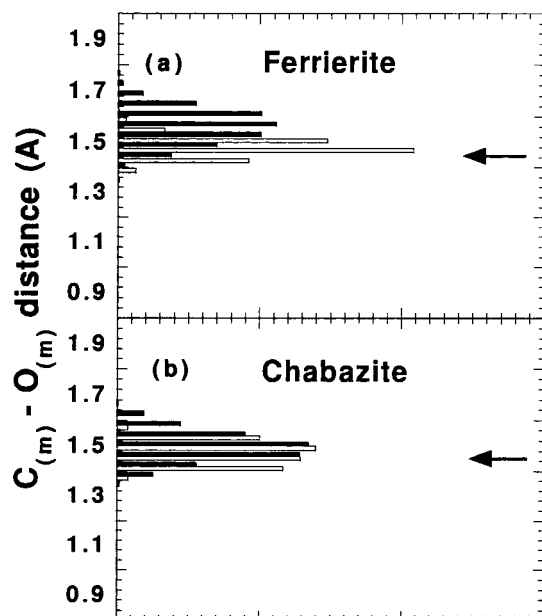

Figure 9. Bond length distributions of the $C-O$ distances in the two-methanol complexes adsorbed in (a) the 8-ring of ferrierite and (b) chabazite. The two distributions in each panel correspond to the methoxonium ion (black) and the methanol molecule (white). The arrows indicate the $C-O$ bond length in the free methanol molecule.

bond manifested by the increase in the anharmonicity of the methoxonium $C-O$ bond shown in Figure 9. However, we find striking differences between the behavior of the two-methanol complexes in chabazite and ferrierite. While in chabazite the protonated methanol chain remains stable (Figure 5e), in ferrierite the chain is broken (Figure 5d) and the two methanol molecules are relatively free to rotate with respect to each other as well as to detach themselves from the acid site. This behavior, studied in more detail in Appendix A, has profound consequences for the process of methanol activation. As can be seen in Figure 9, in chabazite the $C-O$ bond on the methoxonium cation merely undergoes a further increase in anharmonicity with the mean value of the bond length unchanged, while in ferrierite there is a significant shift in the mean value of the $C-O$ bond length (to an average value of ~1.6 Å vs 1.45 Å for the free molecule and showing an elongation of ~15% for about 1.6 ps of the simulation) accompanied by a strongly anharmonic behavior. The activation occurred only for the methoxonium cation and not for the methanol species, hence protonation is a *necessary* condition for the *activation* process. The fact that we observe no activation of the methoxonium cation in chabazite indicates that protonation is *not* a *sufficient* condition. The activation is a consequence of the dynamical behavior of the methanol molecules, which is somewhat reminiscent of the differences in the molecular mobility in the single methanol case. The additional mobility in ferrierite leads to breaking of two H-bonds bonding the methoxonium cation to the methanol cluster and to the framework (Figure 10). The disintegration of the cluster leads to a charge redistribution within the methoxonium cation strengthening the $O-H$ bonds and consequently weakening the $C-O$ bond. Hence, the breakup of the methanol cluster is the *additional factor* needed for activation.

Reaction conditions have been simulated by loading four methanol molecules into the 8-ring channel and associated

(37) A similar effect was observed for methanol in sodalite: Nusterer, E.; Blöchl, P. E.; Schwarz, K. *Chem. Phys. Lett.* **1996**, *253*, 448. Schwarz, K.; Nusterer, E.; Margl, P. *Int. J. Quantum Chem.* **1997**, *61*, 369.
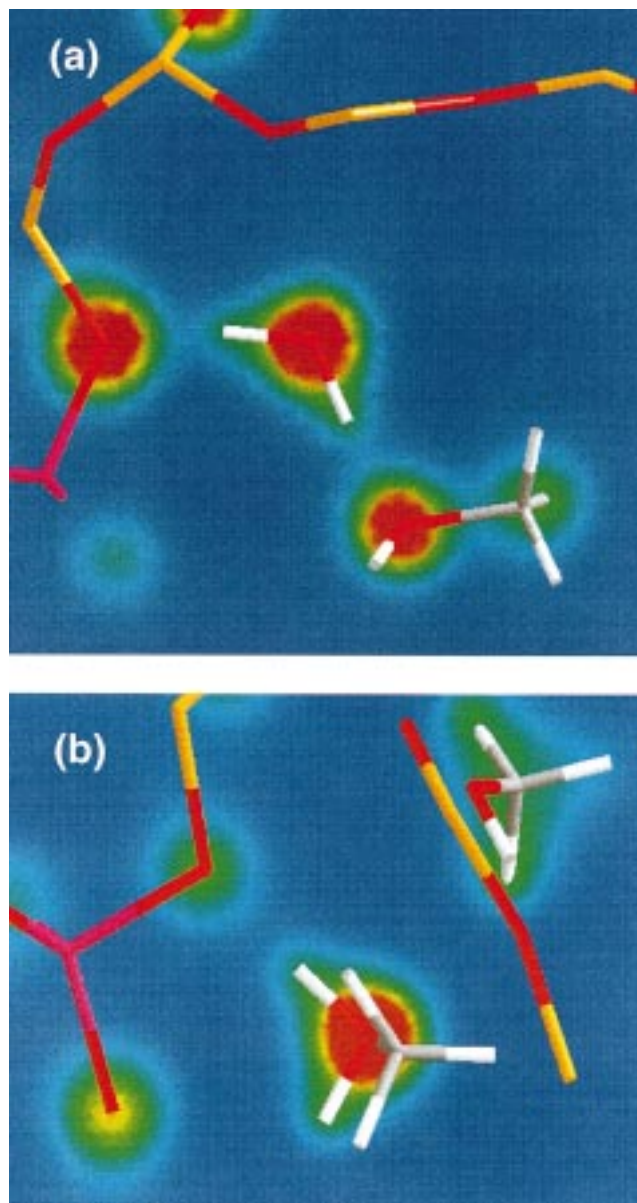
Figure 10. Electronic (valence) charge density on the plane defined by the H−O⁺−H atoms of the methoxonium ion in the two-methanol complexes adsorbed in (a) chabazite and (b) ferrierite. The Al defect is shown in pink. The color scale for the charge densities increases from blue (very low), to green, yellow, and red (very high).

Figure 11. Bond length distributions of the O−H distances in the methoxonium ion in a four-methanol complex adsorbed at $T = 700$ K in the 8-ring of ferrierite. The two distributions correspond to the two protons.

Figure 12. Bond length distributions for the C−O distances in the methoxonium ion (black) and the other two molecules (white) which are not protonated by the proton migration (see text). The arrow indicates the C−O bond length in the free methanol molecule.

Figure 13. Temporal evolution of the square displacement of the center-of-mass displacement of the methoxonium ion.

intersection regions of ferrierite and by increasing the temperature in the simulation to 700 K. Results of the simulations are shown in Figures 11, 12, and 5f. We find that the zeolitic proton is completely transferred to the methanol molecule (Figure 11). The tail in this distribution extending to larger methanol−hydrogen distances now has a completely different origin than in the case of single methanol adsorption in Figure 3. Toward the end of the simulation proton transfer to a nearby molecule started to occur. Hence, unlike in Figure 3 where these fluctuations in the O−H distance were due to a proton moving back to the zeolite framework, the present events represent protons moving between the methanol molecules. Furthermore, we again observe activation of the methoxonium species as evidenced by the significantly stretched C−O bond distribution in Figure 12 with an average value exceeding ∼1.6 Å, and instantaneous bond length fluctuations stretch the length of the bond close to 1.8 Å. The temporal evolution of the methoxonium bonds is shown in Appendix A.
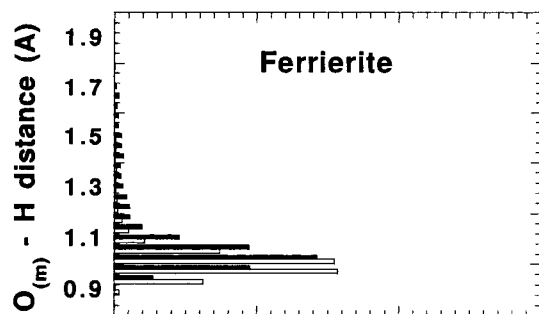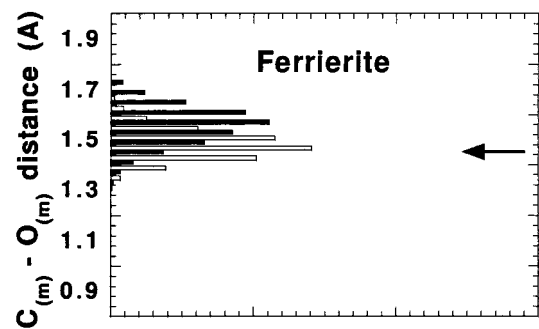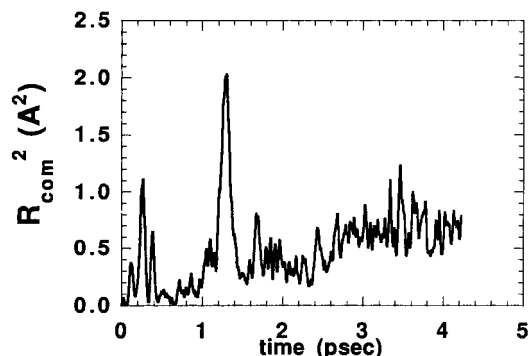
At this temperature the mobility of all the adsorbed species is greatly enhanced. The methoxonium cation is solvated by the other molecules and screened from the acid site. Under these conditions the methoxonium species rotates away from the acid site. To give an impression of the large distances the molecules can travel inside the zeolite framework we show in Figure 13 the temporal evolution of the squared displacement of the center-of-mass of the methoxonium cation

$$R^2_{com}(t) = (\vec{R}_{com}(t{=}0) - \vec{R}_{com}(t))^2 \qquad (5)$$

where $\vec{R}_{com}(t)$ is the position vector of the center-of-mass of the methoxonium cation. The fluctuations result in methoxonium displacements as large as 1.5 Å and the drift we observe toward the end of the simulation means that the molecule has traveled ∼1 Å. Under these conditions the methoxonium ion does not create hydrogen bonds to the other methanol molecules and only occasionally hydrogen bonds to the zeolite framework. Hence,

as in the case of the two-methanol complex in ferrierite, the effect of protonation is *not counteracted* by additional hydrogen bonds leading to the effect of activation.

Vibrational spectra provide the most stringent scrutiny of our results as they can be compared with the measured IR spectra.[2] The difference in the measured vibrational spectra with and without the adsorbed methanol shows at low methanol pressures bands at (3545, 2900, 2440) cm^{-1} assigned to O−H stretches and (2993, 2958, 2856) cm^{-1} assigned to C−H stretches and a band at 1687 cm^{-1}. These results have been interpreted as evidence for the presence of the methoxonium species where the antisymmetric and symmetric O−H vibrations account for the bands at 2900 and 2440 cm^{-1}, respectively, and the O−H bending for the 1687 cm^{-1} feature.[2] At higher methanol pressures, the bands at (2900, 2440) and 1687 cm^{-1} disappear and a new broad band centered around 3325 cm^{-1} and a feature at 1580 cm^{-1} appear. The intensity of the highest frequency band at 3545 cm^{-1} decreases with increasing methanol pressure. The disappearance of the antisymmetric and symmetric stretching vibrations of the O−H groups of the methoxonium ion was attributed to the weak interactions of the methoxonium cation with the methanol solvent.[2]

Information on the vibration of the methanol is contained in the MD trajectories and can be simply obtained by Fourier transforming the velocity autocorrelation function

$$Z(t) \propto \langle \vec{v}(t) \cdot \vec{v}(0) \rangle \tag{6}$$

with $\vec{v}(0)$, $\vec{v}(t)$ being the ionic velocities at initial time and time t and $\langle ... \rangle$ the canonical ensemble average. $Z(t)$ can be computed for any selected atom or group of atoms. We note that this treatment does not rely on the harmonic approximation whose validity is questionable in a regime characterized by strong anharmonicity (cf. Appendix A). We show now that results of our simulations are in qualitative agreement with the experimental IR spectra.

As an example for the single methanol vibrational spectra we show in Figure 14 the results for a single methanol molecule adsorbed in the 8-ring channel of ferrierite along with the positions of the experimental IR bands. As can be seen, the computed spectra are in poor agreement with experiment. There is a noticeable feature in the O−H vibrations at around 1600 cm^{-1} that agrees relatively well with the experimental frequency of the O−H bending mode, but at the experimental frequencies of the symmetric/antisymmetric O−H stretches we find only a featureless background of diverse vibrations extending from ~2000−3500 cm^{-1}. The other disagreement is found in the positions of the C−H stretches which are too high in our calculation. We find similar results also in the other single methanol calculations. The vibrational density-of-states for the case of the two-methanol complex adsorbed in the 8-ring of ferrierite in Figure 15 shows significant improvements over the single methanol case. The weight has been shifted to the region of the experimental symmetric/antisymmetric O−H stretches, the frequency of the O−H bending mode was slightly increased, and the frequency of the high-frequency O−H mode decreased. We note that most of these features are absent in the spectra calculated for the two-methanol complex adsorbed in chabazite (Figure 16), as is the slight downward shift in the frequency of the C−O stretch around ~1000 cm^{-1} (not shown). The experimental spectra at high methanol pressures (taken at room temperature) can be compared with the spectra for our four-methanol complex in ferrierite, shown in Figure 17. Again, qualitative agreement is very good. The symmetric/antisymmetric O−H stretches have vanished as well as the high-
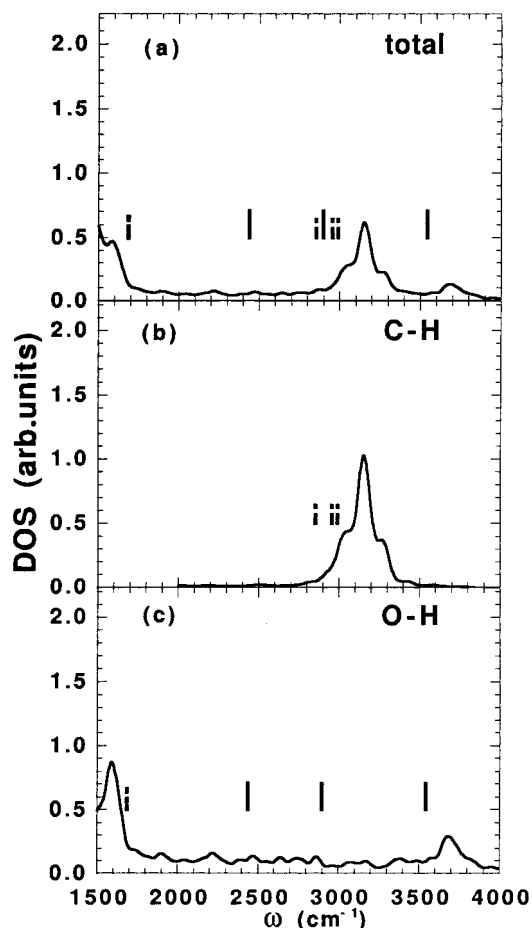

Figure 14. Spectral function for single methanol adsorbed in the 8-ring channel of ferrierite (normalized to $\int_0^\infty Z(\omega) \, d\omega = 1$): (a) total spectra; (b) C−H modes; and (c) O−H modes. The vertical bars correspond to the experimental positions of the IR bands:[2] solid line O−H stretches, dash-dotted line C−H stretches, dotted line O−H bending.

frequency O−H mode and there is a slight downward shift of the O−H bending mode.

These results can be understood as follows. We first observe that, in agreement with the experimental assignments, only the methoxonium cation can produce the O−H modes experimentally observed at (3545, 2900, 2400) cm^{-1} and 1687 cm^{-1}. The symmetric/antisymmetric O−H stretches are missing from the single methanol spectra, which we believe is due to the absence of protonation (chabazite, ZSM-5) or due to too strong interaction of the methoxonium species with the zeolite framework (ferrierite) which causes the downward shift of these frequencies and the diffuse nature of the spectrum (as well as the absence of activation of the methanol molecule). As discussed above, these framework interactions are greatly reduced in the case of the two-methanol complex adsorbed in ferrierite, which causes the overall improvement of the agreement with experiment. This seems to suggest that single methanol complexes are not favored and that methanol may tend to *cluster* even at low loadings. These data also suggest a different interpretation of the 3545 cm^{-1} O−H mode. This band has been interpreted[38] as resulting from −Si−O−CH$_3$ and −Si−OH groups produced by dissociative chemisorption of methanol. We observe the presence of a high-frequency O−H mode when the two-methanol complex

(38) Pelmenshikov, A. G.; Morosi, G.; Gamba, A. *J. Phys. Chem.* **1992**, *96*, 2241.
(39) Tuckerman, M. E. et al. *J. Chem. Phys.* **1992**, *97*, 2635.
(40) Tuckerman, M. E. et al. *J. Chem. Phys.* **1996**, *104*, 5579.
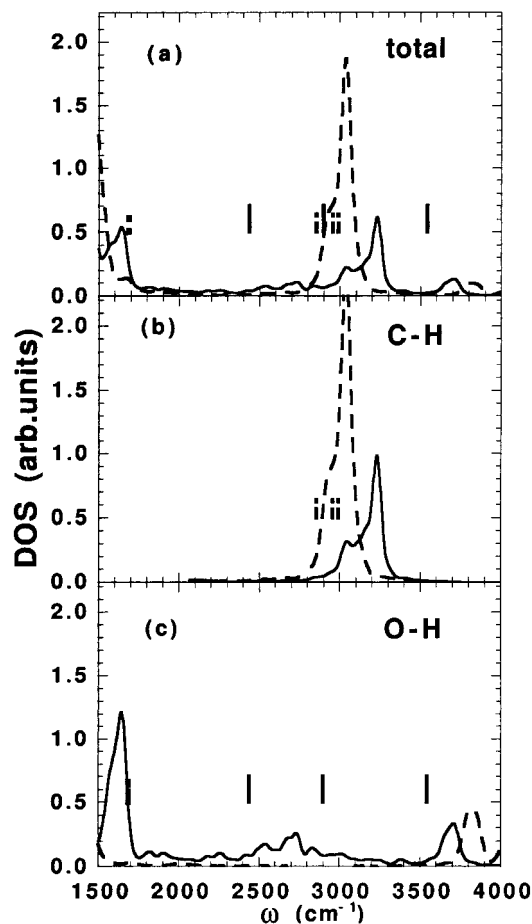(41) Štich, I. et al. *J. Chem. Phys.* **1997**, *107*, 9482.

Figure 15. The same as Figure 14 but for a two-methanol complex adsorbed in the 8-ring channel of ferrierite: solid line methoxonium cation, dashed line methanol.

Figure 16. The same as Figure 15 but for a two-methanol complex adsorbed in chabazite.

is adsorbed in ferrierite and its absence when adsorbed in chabazite. This difference can be traced back to slight differences in the O−H distances in the protonated species in the two cases (cf. Figure 8). In ferrierite, one of the two protons has a slightly shorter average bond length than the other, and hence produces a somewhat higher frequency. This happens especially when the other proton executes a slight fluctuation away from the methoxonium ion which is not the case in chabazite where both protons appear to have equal and slightly larger average bond lengths. This behavior in combination with C−H stretches which are too high leads us to conclude that the protonated hydrogen-bonded cluster of two methanol molecules formed in chabazite is not consistent with experimental data. The behavior at high loading can, in agreement with the experimental assignments, be qualitatively accounted for as resulting from a multitude of very weak interactions which result in the disappearance of the symmetric/antisymmetric as well as the high-frequency O−H stretches. Of course, the very complex nature on the interaction of the species among themselves and with the zeolite channel makes quantitative comparisons with experiment rather difficult.

The model based on our results is as follows. The role of the zeolite framework is to provide the constraint that assists the proton transfer from the active site to the methanol molecule. This produces an increase of the anharmonicity of the methoxonium C−O bond. Solvation of the methoxonium in the methanol solvent leads to a further very significant increase of the anharmonicity and softening of the methoxonium C−O bond. Certain zeolite frameworks play an active role in the solvation process by promoting methoxonium mobility inside the zeolite channel. The activation occurs only if the mobility
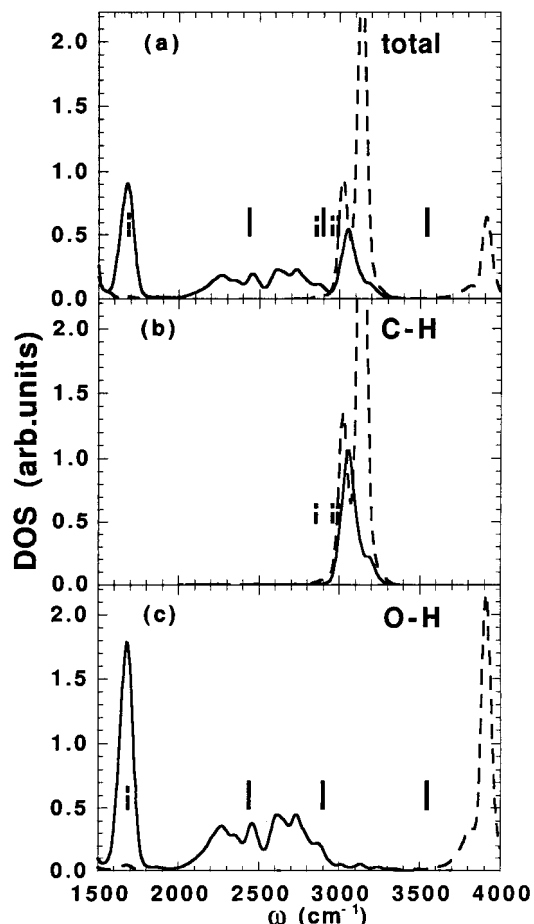
of the methoxonium ion prevents it from forming hydrogen bonds with the acid site and the other methanol molecules. Hence, only the *combination* of the above effects can produce the methoxonium ion in the activated state. This simple model explains the failure to observe activation for a single methoxonium ion in a vacuum and in the zeolite (absence of the methanol solvent), and even at higher loadings in some frameworks (low methoxonium mobility), and the presence of activation under reaction conditions (methanol solvent and high methoxonium mobility).

4. Conclusions

We have presented a very extensive first-principles MD study of the initial adsorption and activation of the methanol molecules in the catalytic environment of microporous aluminosilicates. The central result of the paper is the first observation of an activated methanol species in zeolite catalyst in a theoretical study. A simple model for the activation process is developed. We find that protonation of the methanol molecule and creation of the methoxonium species is only a necessary but not sufficient condition. The methoxonium cation is only activated in methanol solvent and in the case it can be shielded from forming new hydrogen bonds with the other adsorbed methanol molecules and the active site. The conditions under which this combination of factors occurs has been thoroughly studied. The protonation may occur even for a single methanol molecule adsorbed, depending on the zeolite framework. The results indicate that in this early stage of the MTG process the commercial catalyst ZSM-5 does not introduce any new features explaining the activation process. We observed creation of the methoxonium
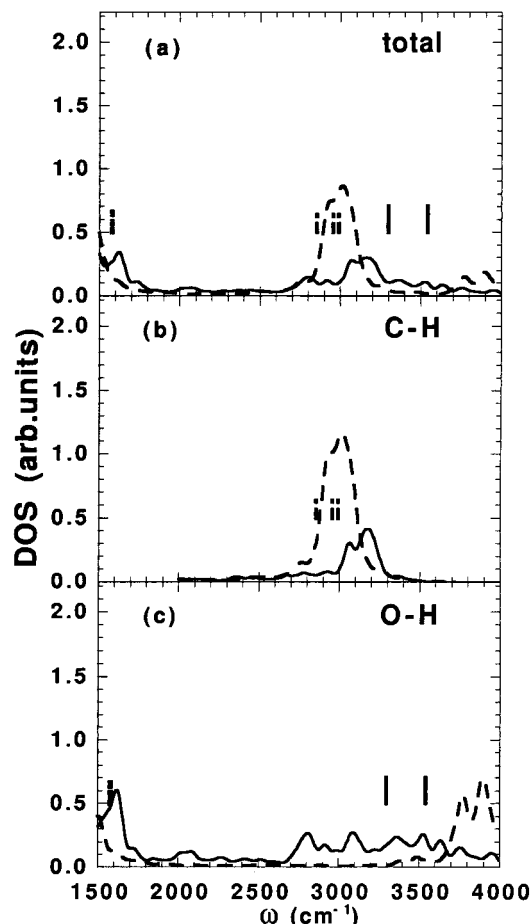
Figure 17. The same as Figure 15 but for a four-methanol complex adsorbed in ferrierite.
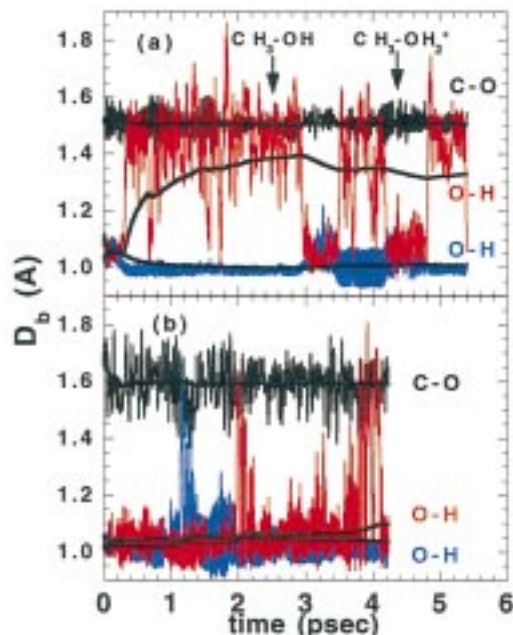

Figure 18. Time evolution of the C−O and O−H bond lengths in (a) one methanol molecule in chabazite and (b) methoxonium cation in the four-methanol complex in the 8-ring of ferrierite. The heavy black lines represent evolving average bond lengths. Some sections of the trajectory in which either methanol or methoxonium ion is present are indicated in part a.

Appendix A: Thermal Fluctuations

In Section 3 we presented the properties of the methanol bonds in integral form. Here we analyze their evolution in time. As an example we show in Figure 18a the evolution of the C−O and the two O−H bonds of the protons closest to the oxygen for the single methanol adsorbed in chabazite. The motion of one of the two protons (red) is characteristic of a motion in a double well potential, with the physisorption well lower in energy than the chemisorption well. The energy barrier for this process must be of the order of ∼5kJ/mol as the proton surmounts the barrier several times on the simulation time scale.

Bond fluctuations under reaction conditions are shown in Figure 18b by the evolution of the methoxonium bonds for the case of a four-methanol complex adsorbed in the 8-ring of ferrierite at 700 K. We see two kinds of proton fluctuations away from the methanol molecule. One (blue) corresponds to an accidental fluctuation of the methoxonium ion back to the proximity of the acid site leading to a proton returning to the zeolite framework. It is interesting to notice that such a process is accompanied by an immediate reduction of the methanol C−O bond. The proton fluctuations occurring later (red) are fluctuations corresponding to proton moving between different methanol molecules. The high degree of anharmonicity of the system under reaction conditions is evident from the huge amplitudes of the bond vibrations which in the case of the proton reach ∼50% of the equilibrium bond length.

Finally, we show in Figure 19 the nature of the fluctuations which lead to activation of the methoxonium ion in the two-methanol complex adsorbed in the 8-ring of ferrierite. One can identify two dynamical events which trigger the activation process shown by the evolution of the C−O bond on the methoxonium ion in Figure 19a. The activation process was started by rotation of one of the two methanol molecules in the cluster (Figure 19b). This led to breaking the hydrogen bond linking the methoxonium ion to the methanol cluster and started
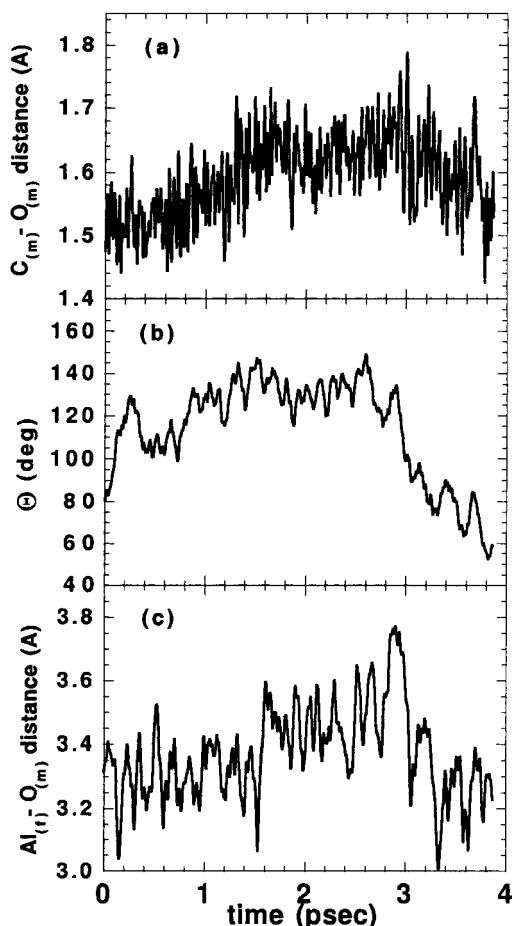
species in all cases studied at methanol loadings of two molecules or higher per acid site. The prevention of forming new hydrogen bonds of the methoxonium species depends critically on the mobility of the protonated species in the zeolite channel which can be enhanced by certain zeolitic environments or simply by raising the temperature to that used in the MTG process. We note that this latter factor was absent in most of the theoretical studies performed to date which relied on the local static optimization and hence were always permitting the formation of the hydrogen bonds counteracting the effect of protonation. This explains the failure to observe the activation process in the previous studies. On the other hand, we found that the quantum dispersion effects appear to have a much weaker effect on the results which are essentially correct within the classical approximation for the protons. Our findings are in qualitative agreement with the measured IR spectra. The strongly activated methoxonium complexes we have observed will be very susceptible to a nucleophilic attack by another methanol molecule and would follow reactions 3 and 4 on a longer time scale. Calculations with constrained reaction coordinate dynamics[42] are now under way.

(42) Carter, E. A. et al. *Chem. Phys. Lett.* **1989**, *156*, 472.

Figure 19. Time evolution of (a) the C—O bond length on the methoxonium cation, (b) mutual angle between the methanol molecules, and (c) the distance between the aluminum defect and the oxygen atom on the methoxonium ion in the case of two methanol molecules adsorbed in the 8-ring of ferrierite.

the activation. This process was further reinforced by breaking also the other hydrogen bond bonding the methoxonium ion to the acid site (cf. Figure 10) as evidenced by the increase of the distance between the oxygen on the methoxonium ion and the aluminum on the zeolite framework at around 1.4 ps in the simulation shown in Figure 19c. This combination of processes produces the strongly activated methoxonium complex we observe in the time interval $(1.4 \div 3.0)$ ps in the simulation.

Appendix B: Quantum Fluctuations

As shown above, proton transfer reactions proceed on a highly anharmonic double-well PES. To investigate the effect of quantum fluctuations in the proton-transfer reaction we have used PIMD techniques.[24,25] We have mapped the canonical integral onto 8 cyclically connected replicas defining the imaginary time axis. This means that *all* protons are treated quantum mechanically. The nuclear exchange was neglected, hence we treat all the protons as Boltzmannons. This description is sufficiently accurate at relatively high temperatures such as
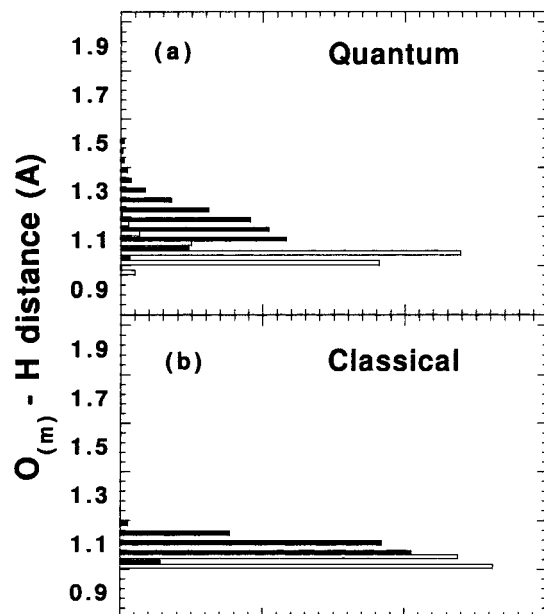

Figure 20. Bond length distributions of the O—H distances for the methoxonium ion with the protons described (a) quantum-mechanically and (b) classically. The two distributions in each panel correspond to the two protons.

those of interest here. The efficiency of the algorithm is increased by using the staging transformation.[39] Due to the stiff harmonic springs connecting the replicas the system is non-ergodic. Ergodicity in our MD calculation was restored by applying chains of Nosé—Hoover thermostats[39] of length 4 separately to each nuclear degree of freedom. Details of the PIMD method and its present implementation are described elsewhere.[40,41] Other parameters of the calculations were taken as given in Section 2.

We have chosen to investigate the proton transfer occurring between two different methanol molecules in the case of the four-methanol complex adsorbed in the 8-ring channel of ferrierite (cf. Section 3). To separate the effect of thermal and quantum fluctuations we have performed two calculations starting from identical initial conditions: (a) a PIMD calculation and (b) calculation with a classical description of the protons. The calculations have been done at room temperature. In both cases after initial equilibration, we have followed the system for ~1500 MD steps. As an example, we show in Figure 20 the distributions of the O—H distance on the methoxonium ion. As expected, the distributions for protons described quantum mechanically are broader than those for classical protons. In particular, the proton attempting to make the transfer to the other methanol is less tightly bonded than its classical counterpart. However, this result indicates that at room and higher temperatures the proton transfers are predominantly thermally activated and the quantum fluctuations represent only a much smaller correction. Hence, we conclude that the *classical* description of the protons is essentially *correct*.